A static fatigue constitutive law for joints in weak rock

Mark K. Larson
Spokane Research Laboratory, National Institute for Occupational Safety and Health, Wash., USA

ABSTRACT: A constitutive model for rock interfaces based on the principles of static fatigue is proposed. The model is applicable to weak rock or joints with cohesion. Friction and dilation are decreased as plastic work increases. At equilibrium, the creep time increases by one time-step interval, and interface cohesion at each node decreases according to a power function. A constant-load, direct-shear simulation showed that the model is capable of mimicking constant-rate and tertiary creep and predicting failure. Tests on core from a coal mine showed constant-rate and, sometimes, tertiary creep, but also weak transitory creep. The cohesion deterioration function may need modification to simulate primary-phase creep. If model parameters are known for a site, the model can predict the onset of tertiary creep and failure. Such predictions can help engineers make better entry design and support decisions, which will reduce the likelihood of roof falls and increase safety for underground miners.

1 INTRODUCTION

Researchers from the Spokane Research Laboratory of the National Institute for Occupational Safety and Health (NIOSH) are developing numerical modeling tools to forecast time-dependent deformation around coal mine entries. Conditions such as weak, layered strata sometimes cause deformation rates to increase so that the roof eventually fails, possibly resulting in injuries and fatalities. Therefore, efforts have been focused on developing models that simulate time-dependent deformation at joints and other planes of weakness. Such models may be applied to other problems, such as slope stability, tunneling, and mining problems involving weak joints.

Most time-dependent interface models are of the viscous-creep type. The rate of slip at some location along an interface is considered to be a continuous (nonlinear) function of the shear stress. Often, therefore, friction, dilation, and cohesion are weakened by displacement and are coupled with the creep model, as Fakhimi (1992) did in his discontinuum model.

In this paper, the principles of static fatigue, or stress corrosion, are applied to cohesion along planes of weakness or joints. The goal is to describe time-dependent mechanisms involving reduction of cohesion coupled with weakening of friction and dilation caused by displacement. This idea seems reasonable because micromechanisms of static fatigue and creep are similar. For example, microcracking is the principal underlying process causing rock creep and static fatigue. Also, both static fatigue and creep rates are affected by temperature and the presence of corrosive agents, such as water. Finally, preliminary modeling of a coal mine site suggested that reductions in joint interface cohesion play a significant role in deformation of strata over time.

2 STATIC FATIGUE

2.1 *Points from the literature*

Wawersik (1974) tested intact and jointed rock specimens (Westerly Granite and Navaho Sandstone) in uniaxial and triaxial compression. Creep of the rock was observed, particularly when water was present. Very little creep was seen in a specimen with a clean, interlocked joint. Based on these tests, Wawersik concluded that creep of jointed rock follows the same general behavior as that of intact material, but with larger amounts of shearing strain for jointed rock.

Charles (1958) conducted investigations of static fatigue in soda-lime glass. He assumed that surface

flaws grow by corrosive interactions between water vapor and components of the glass and that the rate of this reaction is determined by local stress conditions and temperature, pressure, and composition of the atmosphere. To simulate subcritical crack growth in a sliding crack model, Kemeny (1991) used the empirical Charles power law,

$$\dot{c} = c_0 e^{\left(\frac{-H}{RT}\right)} K_I^n, \quad (1)$$

where $\dot{c}$ is crack velocity, H is activation enthalpy, R is gas constant, T is absolute temperature, K_I is mode I stress intensity factor, and c_0 and n are constants.

Several tests and studies of the behavior of intact, brittle, crystalline rock under static fatigue have been conducted. Scholz (1972) and Martin (1972) investigated static fatigue and crack growth in quartz. Each proposed, based on their experiments, that static fatigue might be described by

$$t_f = t_0 P^{-\alpha} e^{\left(\frac{E}{RT} - K\sigma\right)}, \quad (2)$$

where t_f is time to failure, P is partial pressure of water in cracks, E is activation energy for the fatigue process, σ is differential stress, R is gas constant, T is absolute temperature, and t_0, α, and K are empirical constants.

Lajtai et al. (1987) tested specimens of granite in direct contact with water and observed a decrease in strength. Lajtai and Schmidtke (1986) tested specimens of granite and anorthosite in which specimen strength decreased to about 60% of its dry, short-term strength in tests lasting from a few minutes to 17 days. The conclusions from these tests were that (1) creep occurs principally because of microcracking; (2) crack tip strength, long-term strength, and, sometimes, short-term strength are decreased by increasing temperature or by the presence of moisture, while creep strain rate and slow crack velocity are increased; (3) creep rate is dependent on the applied stress-to-strength ratio; (4) in creep tests, crack growth is limited by the rate at which corrosive agents can decrease crack tip strength; and (5) other internal surfaces, such as grain boundaries, pores, and preexisting cracks, also promote crack development.

Price (1964) studied time-dependent strain of coal-measure rocks (Pennant Sandstone, calcareous sandstone, sandstone, siltstone, and nodular, muddy limestone) using bending and compressive creep tests. He could describe the time-deflection results of the bending tests with a Bingham-Voigt model. For heterogeneous rock types, expansion of specimens under constant compressive load can be explained in terms of the release of pockets of residual strain energy formed during the rock's geologic history. He suggested that cohesion among components breaks down during a creep test, thus releasing localized concentrations of strain energy.

2.2 *Mathematical formulation of model*

From the previous subsection, modeling a single plane of weakness with an interface that initially has nonzero cohesion and deteriorates over time according to some function appears reasonable. From equations 1 and 2, dependent parameters might include pore pressure, temperature, activation energy for the fracturing process, and stress level or stress intensity. Although the former three parameters may be significant, for ease of demonstration in this paper, only a measure of stress level will be used as a dependent factor.

Displacement-weakening friction and dilation are likely to be important processes. Therefore, a form of these processes is included in this formulation. What follows is a mathematical description of the model.

Incremental displacements normal and parallel to the joint are represented by

$$\Delta u_n = \Delta u_n^e + \Delta u_n^p \quad (3)$$

and

$$\Delta u_s = \Delta u_s^e + \Delta u_s^p, \quad (4)$$

where Δu_n and Δu_s are relative normal and shear increments of displacement, respectively, and the superscripts e and p refer to the elastic and plastic components of displacement.

The normal (σ_n) and shear (σ_s) stress increments are

$$\Delta\sigma_n = K_n \Delta u_n^e \quad (5)$$

and

$$\Delta\sigma_s = K_s \Delta u_s^e, \quad (6)$$

where K_n and K_s are normal and shear stiffnesses.

The yield function is

$$f = |\sigma_s| + \sigma_n \tan(\phi) - C \quad (7)$$

and the plastic potential function is

$$g = |\sigma_s| + \sigma_n \tan(\psi). \quad (8)$$

C, ϕ, and ψ are mobilized cohesion, friction angle, and dilatation angle, respectively.[1] The plastic components of the relative displacements follow the flow rules

$$\Delta u_n^p = \lambda \frac{\partial g}{\partial \sigma_n} = \lambda \tan(\psi) \quad (9)$$

and

$$\Delta u_s^p = \lambda \frac{\partial g}{\partial \sigma_s} = \lambda \, sgn(\sigma_s). \quad (10)$$

where λ is a scalar multiplier (not a constant) determined by requiring that the new stress point be located on the shear yield surface.

Incremental plastic viscous work is

$$\Delta W_p = \sigma_s \Delta u_s^p - \sigma_n \Delta u_n^p. \quad (11)$$

ϕ and ψ are based on plastic work, such as

$$\phi = \phi_{re} + (\phi_p - \phi_{re}) \, e^{-\alpha W_p} \quad (12)$$

and

$$\psi = \psi_p \, e^{\left[-\left(\frac{W_p}{W_{sl}}\right)^2\right]}, \quad (13)$$

where ϕ_{re} is residual friction angle, ϕ_p is peak friction angle, ψ_p is peak dilation angle, and W_{sl} is an empirical constant.

Cohesion is represented as a combination of residual and time-dependent components, so that

$$C(t) = C_{re} + C_{SF}(t,S), \quad (14)$$

where C_{re} is the residual (i.e., constant minimum value) cohesion, $C_{SF}(t,S)$ is the static fatigue component of cohesion that deteriorates over time, t is time, and S is a safety factor. Various functions are possible to represent the time-dependent change in C_{SF}. One structure for such a function could be represented incrementally according to

$$\Delta C_{SF} = -h(S, C_{SF}) \, \Delta t, \quad (15)$$

where $h(S, C_{SF})$ is an empirical function appropriate for the joint or plane of weakness. For demonstration purposes, in this paper the author has chosen the function

$$h(S, C_{SF}) = C_{SF} \, S^{h_1}, \quad (16)$$

where

$$S = \frac{-\sigma_n \tan(\phi) + C}{|\sigma_s|}, \quad (17)$$

and h_1 is an empirical constant. If S is calculated to be less than 1.0, it is set equal to 1.0.

It is recognized that even if the function, h, can successfully simulate deterioration of cohesion for a constant set of environmental condition, a change in environmental conditions may make any parameter of the function variable or may make the function invalid.

3 CODING OF THE MODEL

The finite-difference code, FLAC, was selected as a vehicle to code the model because of the embedded computer language, FISH, and access to FLAC's internal data array. Several FISH functions were written to overwrite the interface calculation task in the main cycle loop. This is accomplished in three steps. First, interface interaction forces and out-of-balance forces are saved in memory before FLAC executes the interface calculation step. Second, the new interface forces are calculated and saved in place of those forces calculated in the regular interface calculation step. Third, these forces are added to the previously saved out-of-balance forces. Friction and dilation are updated as the solution steps toward equilibrium. At equilibrium, a creep time is increased by the time-step interval, and the cohesion is updated.

A purely elastic case was selected for a test. The case was run with and without the FISH functions. Any differences between the equilibrium states were

[1] The sign convention for stress is positive for tension.

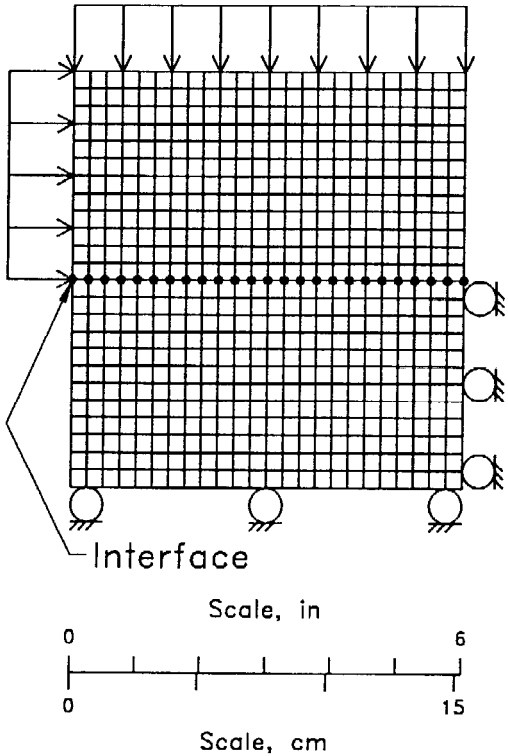

Figure 1.—Direct-shear model grid and boundary condition locations

small, and further experiments showed them to be within the computational precision of FLAC.

A purely elastic case was selected for a test. The case was run with and without the FISH functions. Any differences between the equilibrium states were small, and further experiments showed them to be within the computational precision of FLAC.

4 MODEL DEMONSTRATION

A direct-shear test was simulated in a preliminary demonstration of the model. Figure 1 shows the model grid and boundary conditions. A normal stress of 3.45 MPa (500 psi) was applied for all tests. Friction and dilation angles were initially at 30° and 10°, respectively. Initial cohesion was 1.38 MPa (200 psi), so that initial shear strength was 3.37 MPa (489 psi). Constant shear stresses of 2.09, 2.41, 2.59, 2.76, 2.93, 3.10, and 3.28 MPa (300, 350, 375, 400, 425, 450, and 475 psi) were applied.

Figure 2 is a plot showing x-direction displacements of three points over creep time up to a maximum of 4000 hours. These three points are on the upper half of the interface, that is, the left-most, center, and right-most grid points. Within 4000 hours, tertiary creep and failure set in to all but the two cases with the lowest shear stress. The figure shows some early transitory creep, but not like a classic decaying

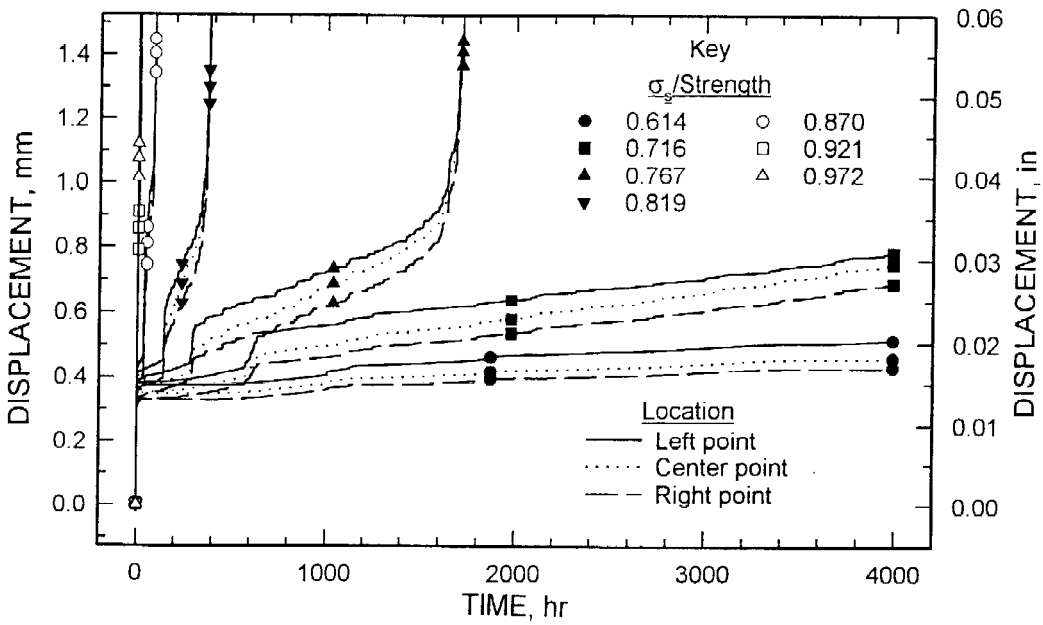

Figure 2.—X-direction displacement versus creep time as calculated by FLAC model with static fatigue FISH functions for various initial shear stress-to-shear strength ratios. Symbols are data points selected to distinguish between sets of lines.

primary-phase creep. Constant-rate creep seems to predominate until tertiary creep takes over. Perhaps primary creep may be simulated by choosing another function for h, possibly in which time, instead of just time step is a direct variable.

An interesting result comes from an examination of the progression of cohesion deterioration in the case where the σ_s-to-strength ratio is 0.716. Figure 3 plots cohesion by location along the interface (left to right) after 4000 hours of creep time. If cohesion deterioration represents the degree of microcracking, then it is evident that microcracking was prevalent on the left side of the interface but did not progress completely across the interface or plane of weakness.

Another observation was that if the σ_s-to-strength ratio is low enough, failure will never occur. No case was run that showed no deterioration, but it is not hard to see that, for practical purposes, this statement is true.

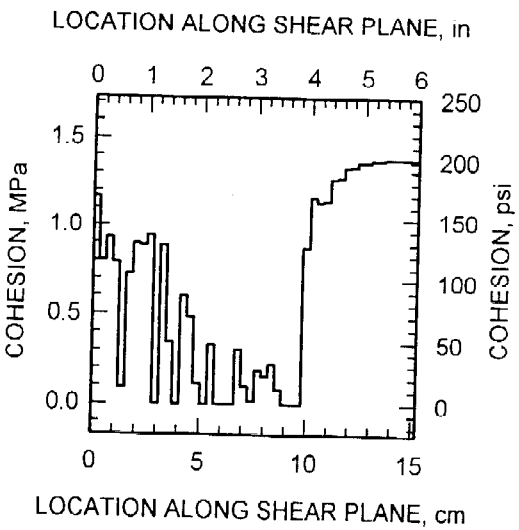

Figure 3.—Cohesion along interface at 4000 hr for σ_s/strength = 0.716

5 COMPARISON WITH LABORATORY TESTS

Larson and others (1995) and Larson and Maleki (1995) reported measurements of roof deformation over time at two sites in a western U.S. coal mine. The roof consists of a carbonaceous mudstone having weak planes throughout along bedding. At site 1, primary-phase creep was prevalent, whereas secondary-phase creep dominated at site 2. Several 152-mm-diameter (6-in-diameter) cores were taken from the roof near site 1. Several direct-shear tests were conducted at the laboratory. The shearing plane was not selected according to any observed plane of weakness, but according to convenience of sample length to the specimen frame.

Figures 4 and 5 are samples of the results of these tests. Figures 4*A* and 5*A* show the history of loading, where a negative value is an applied compressive stress. Figures 4*B* and 5*B* show the history of relative displacement measured on different sides of the specimen (near and far) and an average of the two. Secondary creep was present and predominated in both cases. Primary creep is shown in Figure 5b and may be shown in Figure 4b, but lack of measurement points makes it difficult to confirm. In the case of higher shear stress, tertiary creep and failure resulted just before 550 sec. In the other case, failure had not occurred at 48 hours.

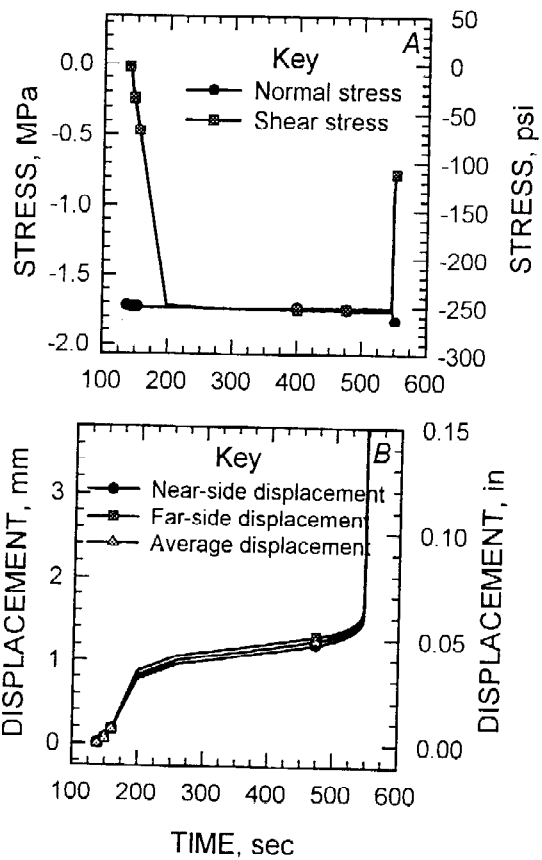

Figure 4.—Results of direct-shear tests on mudstone sample 02. Symbols are data points selected to distinguish between lines. *A*, Normal stress and shear stress over time; *B*, average and relative shear displacement of points on near and far sides of specimen over time.

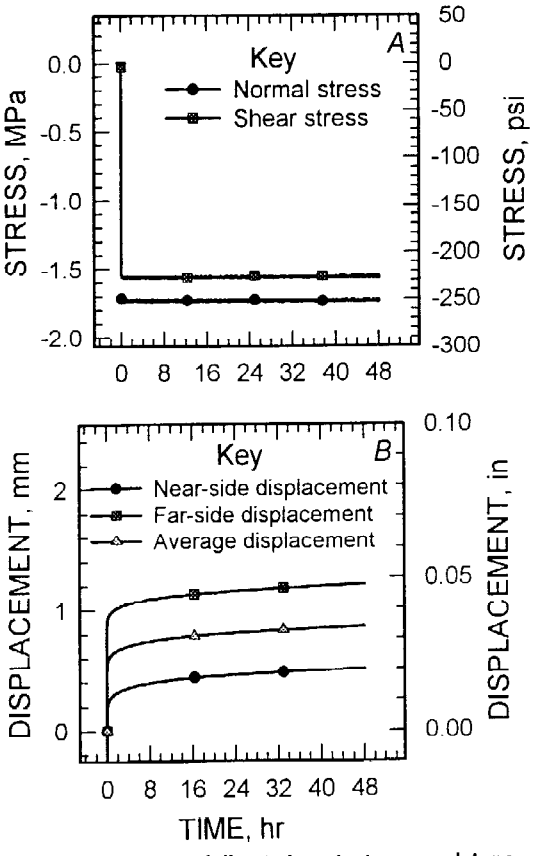

Figure 5.—Results of direct-shear tests on mudstone sample 03. Symbols are data points selected to distinguish between lines. *A*, Normal stress and shear stress over time; *B*, average and relative shear displacement of points on near and far sides of specimen over time.

The deformational curves from the mudstone samples have similar characteristics to the curves from the numerical model. The failure of the model to simulate transitory creep may be remedied with the choice of another cohesion deterioration function, but may not be necessary when predicting the time of failure unless transitory creep is judged to be an important part of the mechanics.

Further tests are planned in which deformation of coal mine roof and slopes will be simulated. Comparisons with real measurements will provide a good measure of the ability of the model to predict time of failure.

6 CONCLUSIONS

The mathematical formulation of cohesion reduction coupled with friction and dilation weakening has been successfully coded with FISH functions in FLAC. Preliminary direct-shear tests show the model appears to simulate progression of microcracking along a plane of weakness. Comparison of these test results with laboratory direct-shear tests of core taken from a coal mine roof shows similar creep curve characteristics. Secondary creep can be reasonably simulated, but primary creep simulation would likely require adjustment of the cohesion deterioration function.

Further tests must be executed to evaluate the capability of the model to simulate deformation and failure over time in the field.

ACKNOWLEDGMENTS

The author is grateful to Jeffrey K. Whyatt, mining engineer, Spokane Research Laboratory, for many useful discusions in the development of the model. Cheng Ho Lee, formerly with Itasca Consulting Group, provide initial guidance in writing FISH functions. Christine Detournay, of Itasca Consulting Group, provided information that aided in debugging the functions. Karen Walker, a student at Gonzaga University, Spokane, WA, assisted with the laboratory tests and data reduction.

REFERENCES

Charles, R. J. 1958. Static fatigue of glass. *J. Applied Phys.* 29 (11):1549-1560.

Fakhimi, A. A. 1992. *The Influence of Time Dependent Deformation of Rock on the Stability of Underground Excavations*. Ph. D. dissertation, Univ. Minnesota, 186 pp.

Kemeny, J. M. 1991. A model for non-linear rock deformation under compression due to sub-critical crack growth. *Int. J. Rock Mech. Mine. Sci. & Geomech. Abstr.* 28(6): 459-467.

Lajtai, E. Z., and R. H. Schmidtke1986. Delayed failure in rock loaded in uniaxial compression. *Rock Mech. Rock Eng.* 19(1):11-25.

Lajtai, E. Z., R. H. Schmidtke, and L. P. Bielus 1987. The effect of water on the time-dependent deformation and fracture of a granite. *Int. J. Rock Mech. Min. Sci. & Geomech. Abstr.* 24(4):247-255.

Larson, M. K., C. L. Stewart, M. A. Stevenson, M. E. King, and S. P. Signer 1995. A case study of a deformation mechanism around a two-entry gate road system involving probable time-dependent behavior. In S. S. Peng (ed.), *Proceedings of the Fourteenth International Conference on Ground Control in*

Mining, pp. 295-304. Morgantown, WV: West Virginia Univ.

Larson, M. K., and H. Maleki 1996. Geotechnical factors influencing a time-dependent deformation mechanism around an entry in a dipping seam. In L. Ozdemir, K. Hanna, K. Y. Haramy, and S. Peng (eds.), *Proceedings, 15th International Conference on Ground Control in Mining*, pp. 699-710. Golden, CO: Colorado School of Mines.

Martin, R. J., III, 1972. Time-dependent crack growth in quartz and its application to the creep of rocks. *J. Geophys. Res.* 77(8):1406-1419.

Price, N. J. 1964. A study of time-strain behavior of coal-measure rocks. *Int. J. Rock Mech. Min. Sci. & Geomech. Abstr.* 1(2):277-303.

Scholz, C. H. 1972. Static Fatigue of Quartz. *J. Geophys. Res.* 77(11):2104-2114.

Wawersik, W. R. 1974. Time-dependent behavior of rock in compression. In *Advances in Rock Mechanics: Reports of Current Research, Themes 1-2. Proceedings of the Third Congress of the International Society for Rock Mechanics*, Vol. II, Part A, pp. 357-363. Washington, D.C.: National Academy of Sciences.